

Effect of perforation patterns on the fundamental natural frequency of microsatellite structure

Ahmad M. Baiomy^{*1,2}, M. Kassab², B.M. El-Sehily¹ and R.M. El-Kady¹

¹Mechanical Engineering Department, Faculty of Engineering, Al Aazhar University, Cairo, Egypt

²Egyptian Space Agency, Cairo, Egypt

(Received March 31, 2023, Revised May 7, 2023, Accepted May 26, 2023)

Abstract. There is a burgeoning demand for minimizing the mass of satellites because of its direct impact on reducing launch-to-orbit cost. This must be done without compromising the structure's efficiency. The present paper introduces a relatively low-cost and easily implementable approach for optimizing structural mass to a maximum natural frequency. The natural frequencies of the satellite are of utmost pertinence to the application requirements, as the sensitive electronic instrumentation and onboard computers should not be affected by the vibrations of the satellite structure. This methodology is applied to a realistic model of Al-Azhar University micro-satellite in partnership with the Egyptian Space Agency. The procedure used in structural design can be summarized in two steps. The first step is to select the most favorable primary structural configuration among several different candidate variants. The nominated variant is selected as the one scoring maximum relative dynamic stiffness. The second step is to use perforation patterns reduce the overall mass of structural elements in the selected variant without changing the weight. The results of the presented procedure demonstrate that the mass reduction percentage was found to be 39% when compared to the unperforated configuration that had the same plate thickness. The findings of this study challenge the commonly accepted notion that isogrid perforations are the most effective means of achieving the goal of reducing mass while maintaining stiffness. Rather, the study highlights the potential benefits of exploring a wider range of perforation unit cells during the design process. The study revealed that rectangular perforation patterns had the lowest efficiency in terms of modal stiffness, while triangular patterns resulted in the highest efficiency. These results suggest that there may be significant gains to be made by considering a broader range of perforation shapes and configurations in the design of lightweight structures.

Keywords: design optimization; finite element analysis; microsatellite; modal analysis; structural design

1. Introduction

The cost of launching a satellite system into orbit can be divided into several contributing costs, the major one is its total wet mass at launch -total wet mass is the sum of the total mass of the satellite itself, including all subsystem components and the mass of any fuel placed onboard according to Heidt *et al.* (2000). Hence, the main motivation for the structural design process of small satellites is the reduction of structural mass as much as possible, which directly reduces the launch cost.

According to Sweeting (2018), Kramer and Cracknell (2008), Xue *et al.* (2008), and other

*Corresponding author, E-mail: ahmadmostafa.2114@azhar.edu.eg

sources, the prevailing trend in satellite design is to focus on what are known as “small satellites”. Small satellites are typically categorized according to their weight into: Microsatellites with weight within the 10-100 kg range, Nanosatellites with weight within 1-10 kg range, Pico-satellites with weight within 0.1-1 kg range, and more recently Femto-satellites with weight less than 100 g. For satellites falling in the range of nanosatellites and lower classifications, the primary method of mass reduction is to implement perforations in the structural design, thus reducing structural mass with the removal of material. This has led to the standardized structural design of the so-called 1U, 2U, and 3U CubeSat structures, which were first proposed by Heidt *et al.* (2000) and have since been adopted as an ISO standard for nanosatellites. While for a higher weight range of small satellites, typically classified under the microsatellite category several methods are used to optimize the structural mass according to Larson (1995).

A cluster of three Microsatellites was designed by Horan *et al.* (2002) and delivered in 2002 as a part of the US Air Force University Nanosat program. They used Isogrid theory described in the Isogrid Design Handbook by Meyer (1973) to design the structure. The structure for each satellite was manufactured from a machined 6061-T6 aluminum isogrid structure according to Abdel Hamid (2022).

The adoption of new technologies, especially COTS (Commercially On The Shelf) devices, has enabled the rapid development of small satellites with high utility at low cost. Small satellites are changing the Earth observation/remote sensing and digital communications space business through machine-to-machine exchanges, linking the Internet of Things with big data warehouses and AI data mining.

When creating a structural subsystem for a satellite, it's crucial to focus on reducing its weight. Drenthe *et al.* (2019) conducted research that sheds light on the cost effectiveness of smaller commercial launch systems in the era of collaborations between public and private entities in spaceflight. This information can help the aerospace industry make important design decisions early on. They stated that the satellite's weight determines the choice of launcher, and launch costs are directly proportional to the launcher's class.

Jones (2018) provided information indicating that the cost of launching a single kilogram into a low Earth orbit, which is between 200-2000 km above the Earth's surface, is approximately \$2720/kg for the widely used SpaceX Falcon 9 launch system. Therefore, reducing the mass of any satellite can result in significant cost savings for the space program.

The launch providers impose another crucial requirement on satellite design, which is to ensure that the satellite's fundamental natural frequency (referred to as FNF) is significantly different from the launcher's critical natural frequency. This modal parameter is given utmost importance since launch service providers explicitly specify this critical value in their user manuals, such as Spaceflight, Inc.'s mission planning guide (2019). The purpose of this requirement is to prevent the satellite's FNF, which can be stimulated due to the highly dynamic launch loads, from coinciding with any of the launcher's natural frequencies, resulting in mutual resonance which may lead to the loss of the launcher and its payloads, as highlighted by Garcia-Perez *et al.* (2019), and Fakoor *et al.* (2017). Therefore, the optimization of FNF is the primary parameter of interest in the current study for the design options being evaluated. Additionally, modal analysis serves as a gateway to downstream analysis of dynamic loads. Examples of this approach can be found in the works of Wei *et al.* (2017), Liu *et al.* (2019), and other researchers.

To decrease the weight of a satellite, optimization must be made about how its structure is designed. This can involve choosing an appropriate configuration by selecting a proper geometric shape or reducing the number of structural elements needed to keep the structure stable when

under stress. This is known as topology optimization, which is a larger process that aims to achieve goals such as reducing mass by altering the geometry of structural components. Lim *et al.* (2020), Viviani *et al.* (2008), Akl *et al.* (2017) and other many several studies have explored the use of topology optimization to control and reduce the mass of structures.

Sometimes the requirements of a satellite's mission prevent any modifications to its structural design. For example, the placement of the payload in a specific location in relation to Earth may require a specific structural support design. In such cases, selecting lightweight yet strong and stiff materials for the structural subsystem is the unique viable method to reduce the satellite's mass. This ensures that the structural components can withstand the dynamic loads that the satellite will experience throughout its operational life, particularly during the launching phase.

The utilization of innovative materials in structural design has made it possible to attain success in past satellite projects, particularly for bigger systems weighing 30-40 kg or more. Several studies, such as Cho and Ree (2011), Kuo *et al.* (2017), Zhengchun *et al.* (2016), Kwon *et al.* (2021), and others, have outlined the use of composite materials, primarily in the form of honeycomb cores with composite faceplates.

The reason for the extensive use of composite materials in satellite systems is their ability to provide improved mass savings and stiffness characteristics to designers. Nevertheless, incorporating these materials in any design involves significant financial requirements. This is because the expenses associated with design, analysis, and particularly fabrication are high. The elevated cost is a result of the specialized expertise required for effective implementation, as detailed by Centea and Nutt (2016) and by Lester and Nutt (2021) regarding fabrication cost modeling.

Dealing with space qualified composites is costly, especially when factoring in the need for minimal outgassing, which is a critical requirement. Outgassing is the release of certain chemical compounds from the composite in gas form while in orbit due to the vacuum environment. These gas compounds can then deposit onto critical components of the satellite, including imager lenses, resulting in damage, as highlighted by Anwar *et al.* (2015).

Moreover, these materials must meet more rigorous standards than those used for ground-based systems, which adds to the technical difficulty of implementing them efficiently. Furthermore, these materials are relatively expensive compared to standard metals, resulting in an overall increase in costs, as seen in the work of Shama *et al.* (2018). So, the others strongly recommended a price difference of at least ten times between composite materials used in space and aerospace-grade aluminum 6061 alloy stock, which is a commonly used metallic material in satellite structures.

The present study presents a different method for reducing the weight of a small satellite. Rather than relying on advanced materials, the method involves incorporating metal perforations into the satellite's structural subsystem. The approach involves removing material rather than relying on the material's inherent properties and is based on modifying the satellite's configuration. This approach is significantly less expensive than a conventional composites-based approach to mass reduction, with potential program costs being around one-tenth or more of the total cost. Additionally, a major benefit of this approach is that the perforations can be produced through standard, inexpensive machining processes rather than the demanding fabrication processes required for advanced materials.

The idea of incorporating perforations into structural components is not a new concept. The impact of perforations on the natural frequencies of plates, with different shapes and distributions, has been discussed by Cunningham *et al.* (2020), Abdelrahman *et al.* (2019), Ghonasgi *et al.*

(2016), Jeong and Jhung (2017).

In all of the previously mentioned works, it was discovered that when plates were perforated, their stiffness was reduced, leading to a decrease in their natural frequencies. In their research, Almitani *et al.* (2020) examined the impact of perforations on the natural frequencies of multilayered beams and found a similar outcome. They observed that the number of perforations had an inverse relationship with the natural frequencies, as it caused a reduction in stiffness.

Sun *et al.* (2019) investigated the impact of perforations on the aerodynamic flutter of composite wind turbine blades and concluded that incorporating perforations leads to better flutter suppression damping and higher rigidity. Formisano *et al.* (2016) explored the use of perforated structures in civil engineering, particularly in shear panels that serve as bracing devices for seismic-resistant structures. By selecting an appropriate perforation pattern for the shear panels, the building could experience significant shear deflections without excessively compromising its stiffness and ductility. Sailesh *et al.* (2021) researched the effect of perforations on acoustic soundproofing materials and discovered that perforations with variable geometry had a positive impact on soundproofing performance.

A subassembly from the structural subsystem of a conceptual Microsatellite which was designed for earth resources missions was analyzed by Dawood *et al.* (2021) using the perforation approach for mass reduction. A set of perforation geometric patterns were implemented on the subassembly identical planar plates made of Aluminum 6061 for achieving mass reduction, using a milling machine. The FEM was used to compute the fundamental natural frequency (FNF) of the subassembly and their mode shape. Using this approach, they report a 20% of mass reduction approximately from the unperforated case. Although Four perforation shapes were compared to reach the optimum perforation pattern i.e., to maximize FNF for the same mass, these four shapes didn't include the isogrid shape.

In a sequel two articles by Dawood *et al.* (2022), The author proposed an approach involves implementing geometrically shaped, parametrically defined metal perforation patterns on satellite components. The study includes four geometric shapes used in his previous article but with two scale factor and aspect ratio variations, with the change in the structure's natural frequency as the selection criterion. The best pattern achieved a 23.15% mass reduction while maintaining the same fundamental frequency. Dynamic loading analysis showed that the final perforated design outperformed the baseline unperforated design with respect to maximum displacements, maximum Von Mises stresses, and computed margin of safety. The author investigated the responses of a perforated structural subsystem of a conceptual microsatellite to three dynamic launch loads (quasi-static, random, and shock loads) compared to the baseline unperforated version. The results indicate that the structure would successfully survive these loads without developing stresses that would lead to material failure by yielding. The perforation concept was found to have sufficient merit to be further developed towards implementation in future satellite designs.

The present work is a part of Al-Azhar University Satellite project in partnership with the Egyptian Space Agency. The mass budget dedicated to the structural subsystem is 35% of the overall satellite mass. The main objective is to achieve a structural subsystem as dynamically stiff as possible and as lightweight as possible, i.e., to maximize the modal stiffness-to-weight ratio while taking into consideration the manufacturing constraints and cost. To achieve this target, the term "design efficacy" is used to compare the different design variants. The design is considered 'Efficient' when, for given loading conditions, the design uses as little mass of material as possible. We propose two different quantitative comparative measures to quantify the 'Design efficacy'.

So, the paper outlines a procedure for improving the material utilization of the structural subsystem of microsatellites, which involves two-step sequential procedure, first, the layout configuration of the structural subsystem was configured within the constraints of the application requirements (i.e., The locations and fixation of the contained electronic subsystems) and targeting the highest modal stiffness to mass ratio. Then in the second step, we opted out to increase the modal stiffness having achieved the most mass reduction in the first step, by adding perforations into the structure while fixing the mass.

Although there are many factors that affect the design efficacy, the present paper focuses on the effect of 'Perforation pattern shape'. It is an attempt to study how it can be used to enhance the satellite structure. By 'shape' we mean the perforation geometric pattern typically used to minimize a plate mass. But in the present work, the mass is assumed to be fixed and constant for all the studied plates with different perforation patterns. We hypothesize that even with the mass being fixed a perforated plate can be made stiffer by increasing its thickness while perforating it with different shapes. The objective of this step is to find the preferable perforation-thickness combination under the constant mass constraint. To establish a fitness measure to find the improvement in perforation-thickness combination of the microsatellite structure, we adopt a dynamic similitude-based measure. The next section explains the design methodology and terminology adopted in the present paper.

To prevent dynamic coupling between the low-frequency vehicle and satellite modes, it is recommended that the satellite's structural stiffness be designed based on the Launcher loads and frequency requirements. The launcher requirements supplied by EgSA demand that the longitudinal frequency is to be greater than 90 Hz, and the lateral frequencies should be greater than 45 Hz.

2. Design methodology

The design requirements for the micro-satellite were dictated such that the structural subsystem must be confined within the permitted envelope of 362 mm×362 mm×262 mm. The C.G (Center of Gravity) is defined with respect to the spacecraft axes which are passing through the center of the mounting interface with the separation system. The C.G. position in the longitudinal direction (Y axis) should not exceed 131 mm higher than the mounting plane and the C.G. position in the lateral directions (X and Z axes) should be within +5 mm to -5 mm from the longitudinal axis, and vertical axis, respectively. The structural design process began after all data and kinematic properties of the Payload and Bus Subsystems components were determined and known.

The first phase in the design was to construct a computer-aided design (CAD) model of all the components of subsystems using the commercial software SOLIDWORKS. The pertinent data in the construction of the CAD model was each component's mass, volume, center of gravity, and moment of inertia, to simulate the component's effect on the satellite structure during configuration conceptual design, analyses, and virtual tests.

The sizing was the next logical step in the design procedure since it will impose the space constraint on the size of the satellite configuration and accordingly the choice of external shape and partitions based on the constraints and requirements of different organizations involved in the mission.

The next step was to select the optimum material for the primary structure. The metallic panels were selected as the most effective structural design for our project for several reasons. The main

reason of which is the cost since fiber composite structures are expensive to manufacture and require costly structural testing higher than the project cost budget. While the honeycomb sandwich panels require using potted inserts to attach fasteners which creates safety concerns and parasitic mass. The metallic panels are relatively simple to manufacture and pose less demanding safety and testing requirements.

The next step was to choose the best-fit metallic plate. Aluminum 6061 contains magnesium and silicon which strengthens the alloy during tempering process. This alloy was selected to manufacture the spacecraft structure for two reasons. The material is relatively available and economically feasible for a low-budget program. It has a density of approximately 2.7 g/cm^3 which is roughly about one-third of the steel density, tensile strength of 276 MPa, Young's modulus of 68.9 GPa, and Poisson's ratio of 0.33. secondly, aluminum is simple to manufacture and has relatively good workability. Good workability is an important advantage to be considered for a small-budget program, especially with the imposed manufacturing constraints. After settling on the material and primary shape of the structure, the detailed spacecraft configuration design was commenced to locate each component in a proper location, taking into consideration the mass distribution to guarantee an overall C.G. not to exceed 5 mm far from the G.C. (geometric center) and satisfy the rest of other specific subsystems components requirements.

2.1 Configuration and space allocation

The way in which the components can be packaged within the allocated space is a complicated open problem that requires several specific considerations. All components of subsystems must be accommodated inside the structure in a manner consistent with all requirements. It is important to note that some of the subsystems have their own requirements, that must be considered during the configuration design process.

As an open design problem, reaching an acceptable configuration and space allocation required many iterations, every iteration was based on the expanding knowledge base acquired from the previous iteration since the variety of internal structural design and electronic packaging concepts have evolved in conjunction with the generations of configuration.

There are typically three basic types of structural elements used in the present design: dual shear plate, shelf, and skin panel/frame. The dual shear plate design function is mainly for mounting electronics on plates or specially designed boxes. The plates are then bolted to internal and external shear plates which are inserted into the bus structure from the outside. The shelf configuration refers to an arrangement where shelves are attached perpendicular to the axis of a cylindrical spacecraft and provides support for electronics and other components. The skin panel/frame configuration uses the primary structural frame or bus. The faces of the structure are closed with plates that may form part of the load-bearing structure.

To select a suitable structural configuration, a conceptual evaluation was done via normal mode analysis to choose the most suitable configuration among 11 candidates' proposed variants. The analysis was made without subsystems. The shape, the mass, and the FNF for the first three modes of all the candidate variants are considered in the evaluation, the FNF is described in detail in the following sub-section. Normal modes analysis for the undamped free vibrations system is obtained as follows

$$[K - \lambda_i M] \{\phi_i\} = 0 \quad (1)$$

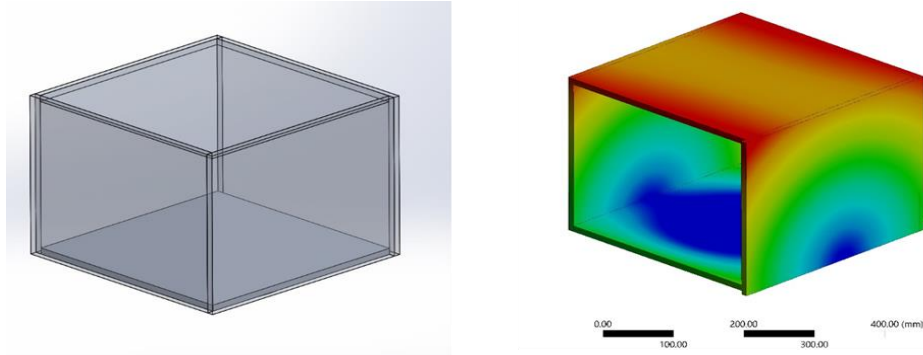


Fig. 1 CAD model and first mode shape of Datum

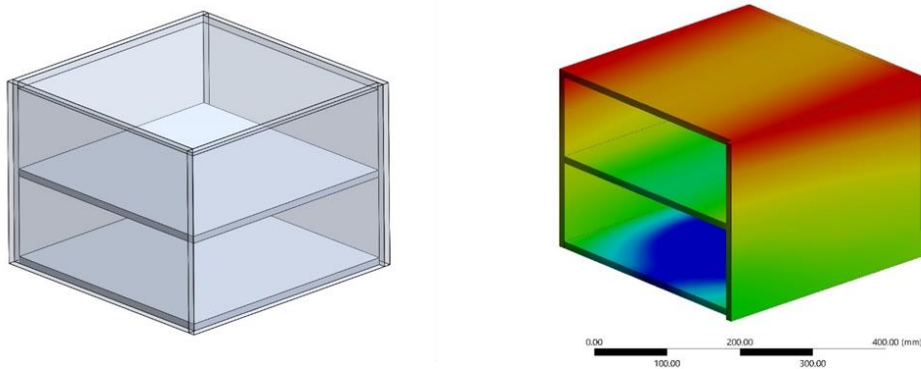


Fig. 2 CAD model and first mode shape of Variant (1)

Where K is the stiffness matrix of the system, M is the mass matrix of the system and λ_i and ϕ_i are to be computed. where λ_i refer to the Eigenvalues and ϕ_i refer to the associated Eigenvector or mode shape. The Eigen values are related to the natural frequencies as follows:

$$f_i = \frac{\lambda_i}{2\pi}$$

2.2 Primary structure configuration

To demonstrate the procedure and establish a reference point to compare the improvements in FNF we started with a very simple configuration variant as the datum. Six plates (10 mm thickness) are used to form a cube, and all subsystems' components are fixed onto the plates. Although this configuration is the most lightweight, the FNF is the lowest. The modal FEA results showed that the first mode shape corresponding to the first FNF appeared in the longitudinal direction. The weak points appeared on the bottom and upper plates, as shown in Fig. 1.

Past studies demonstrated that satellite structure natural frequencies are sensitive to the mass, damping, and stiffness of the structures according to Guo *et al.* (2021). To quantify the improvement through the consecutive variants we used an efficiency quotient defined as

$$I_{variant} = \frac{(FNF_{variant})^2 * (mass_{variant})}{(FNF_{datum})^2 * (mass_{datum})} \quad (2)$$

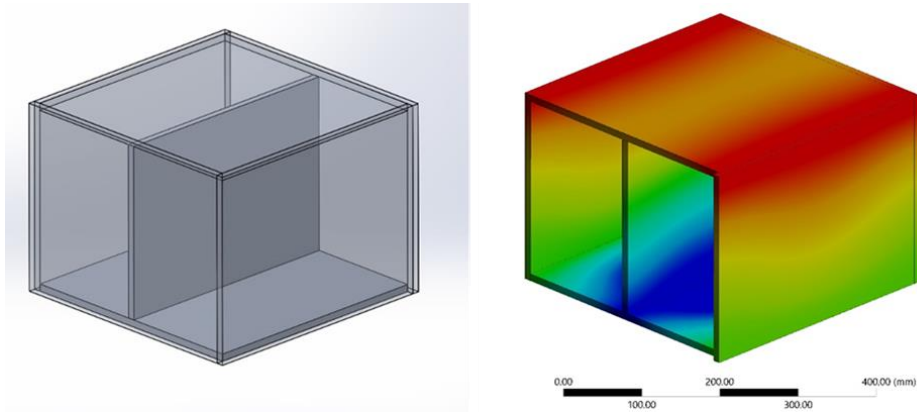


Fig. 3 CAD model and first mode shape of Variant (2)

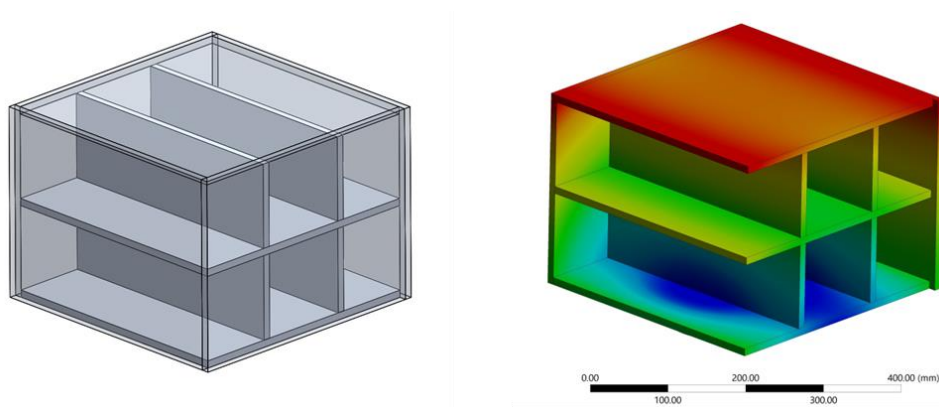


Fig. 4 CAD model and first mode shape of Variant (3)

Such that $I_{variant}$ quantify the change in the “fundamental modal stiffness” either increasing or decreasing over the datum design, i.e., the simple cube according to Oku Topal and Akpinar (2021).

The first variant (variant 1), shown in Fig. 2 incorporates a horizontal mid plate as a shelf to be used in the fixation of subsystems components on both sides. The overall mass increased to 19434.28 grams and FNF slightly increased to achieve $I_1 = 1.13$.

Further, to improve the dynamic stiffness based on mode shapes found in the previous variant, a longitudinal plate instead of the horizontal one in variant 1 was added to stiffen the cube longitudinally as shown in Fig. 3. This led to a higher increase in FNF while resulted in less gain in mass compared to variant 1 scoring an $I_{variant}$ of 1.18. The modal FEA results shown in Fig. 3, revealed the weak spots in the first mode shape appearing on both left and right plates.

In variant 3 shown in Fig. 4, a lateral plate was used as a shelf and a pair of plates were used on both sides to improve both lateral and longitudinal stiffness. This led to a significant increase in both the first FNF and yielded a mass of 23718.85 grams while registering an 8.19 of $I_{variant}$. The size of payload and battery -as they represent the biggest size among all subsystem’s components- was taken into consideration to determine the interspaces between plates within this configuration variant.

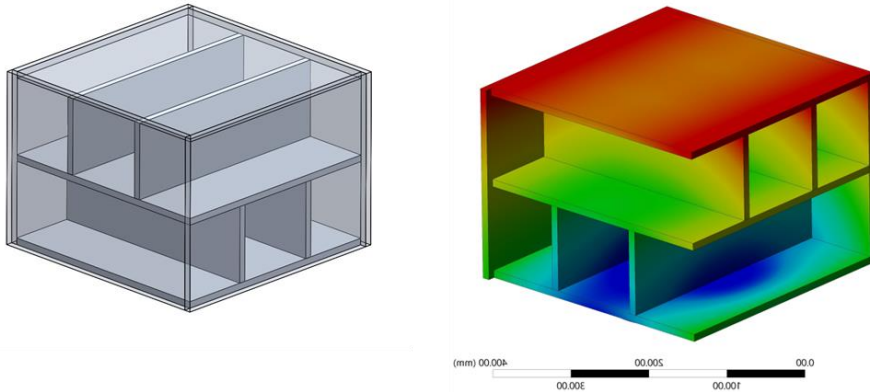


Fig. 5 CAD model and first mode shape of Variant (4)

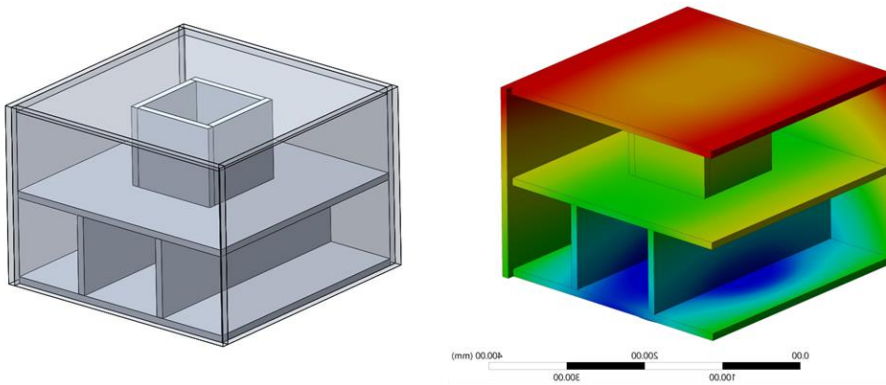


Fig. 6 CAD model and first mode shape of Variant (5)

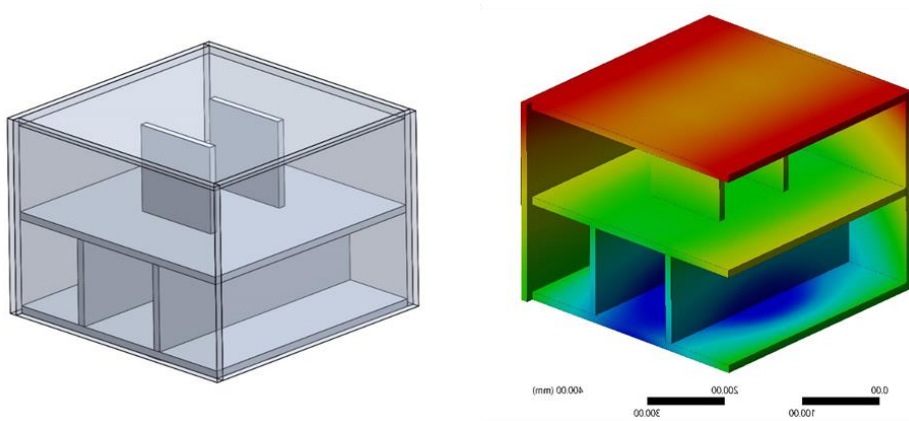


Fig. 7 CAD model and first mode shape of Variant (6)

The next variant 4 shown in Fig. 5, is like the previous one (variant 3), but the two plates were rotated to be perpendicular to their previous orientation. This led to increasing in FNF, while having the same mass achieving 8.34 of $I_{variant}$.

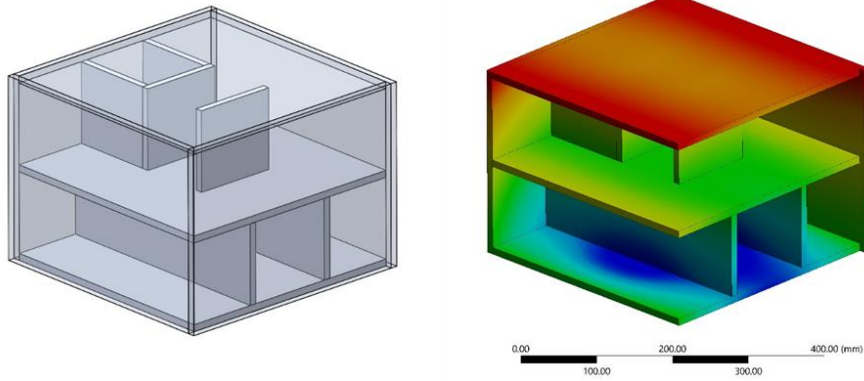


Fig. 8 CAD model and first mode shape of Variant (7)

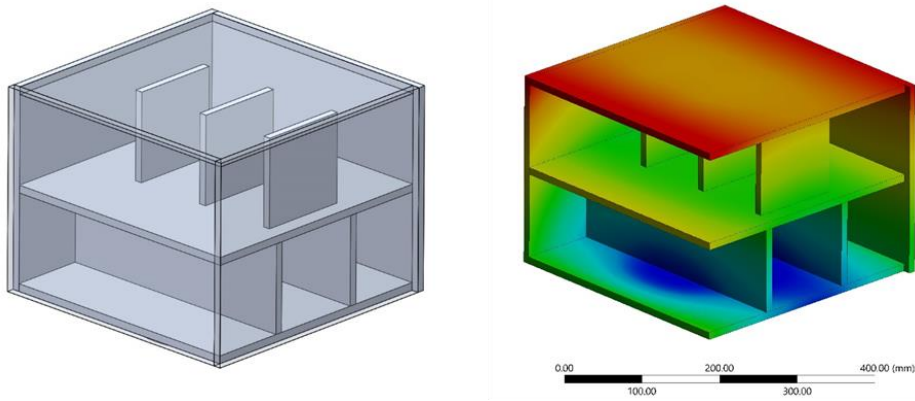


Fig. 9 CAD model and first mode shape of Variant (8)

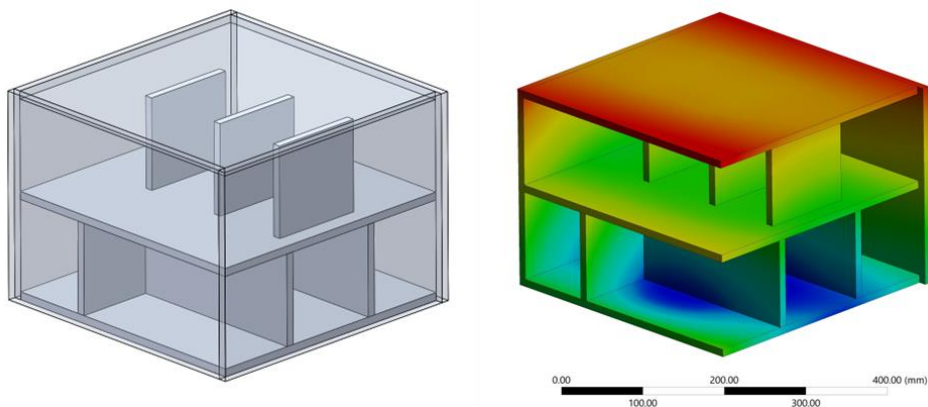


Fig. 10 CAD model and first mode shape of Variant (9)

In variant 5 the upper pair of plates were replaced by four plates smaller in size to form a box as shown in Fig. 6. This led to a reduction in the mass to 23079.92 g, and a little bit of loss in the FNF with $I_{variant} = 8.51$.

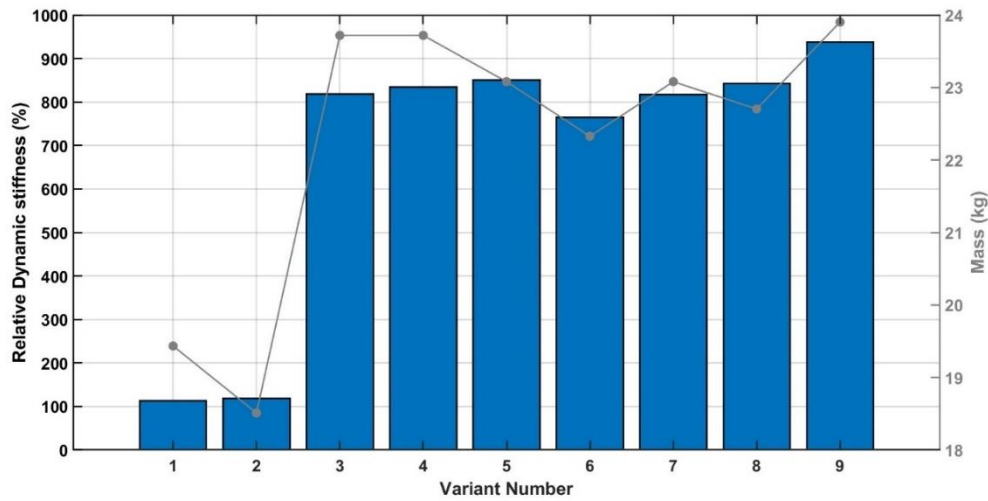


Fig. 11 The percentage relative gain in dynamic stiffness vs the variants

Table 1 Mass, FNF, fundamental modal stiffness, and mesh details of variants

	Mass (g)	FNF	I variant	Mesh density	Element size (mm)
Datum variant	16276.25	142.70	–	60765	5
variant 1	19434.28	138.89	1.13	70287	5
variant 2	18510.88	145.55	1.18	67527	5
variant 3	23718.85	338.38	8.19	83535	5
variant 4	23718.85	341.40	8.34	83535	5
variant 5	23079.92	349.50	8.51	81519	5
variant 6	22328.24	336.90	7.65	79215	5
variant 7	23079.92	342.60	8.17	81519	5
variant 8	22704.08	350.67	8.42	80367	5
variant 9	23902.67	360.60	9.38	82287	5

In variant no 6 shown in Fig. 7, two of the four plates were removed to reduce the mass to 22328.24g, but at the expense of the FNF decreasing to an $I_{variant}$ of 7.65.

Variant no 7 shown in Fig. 8 had a mass of 23079.92 g exactly like variant 5 but with a detrimental effect on the FNF with an $I_{variant}$ of 8.17.

Variant no 8 shown in Fig. 9 achieved 350.67 Hz of FNF with mass 22704.08 g thus obtaining 8.42 as an $I_{variant}$.

Variant no 9 shown in Fig. 10 achieved the maximum FNF with a mass of 23902.67 g and scoring a value of 9.38 for $I_{variant}$.

The results are summarized in Table 1, which also lists the mesh size and element size used in the modal analysis. The percentage relative gain in dynamic stiffness is plotted in the column plot vs the variants plotted in Fig. 11.

3. Perforation study

After establishing the configuration variant 9 as the best candidate with the highest modal

stiffness-to-mass ratio, the question arises could there be further improvement within the constraints of the mass and without altering the primary configuration? And if so, how could the material utilization be quantified? We shall answer the second question first.

3.1 Material utilization indicator

In the engineering design discipline, the use of similitude theory is made for different goals that establish the similarity between a small prototype and the actual design. As shown by Pahl *et al.* (2007), the similitude theory in engineering design is used for the development of size ranges with the objective of achieving the same level of material utilization. Thus, in the present case if we consider two material body configurations; we have a dynamic similitude between the two configurations if the indicator value (N) defined below for both configurations is the same.

$$N = \frac{\rho v^2}{E} \quad (3)$$

Where, ρ and E are the material density and elastic constant of the material of the configuration, while v is the velocity with which the configuration may move under the prescribed boundary conditions.

So, to quantitatively compare two design variants with respect to their material utilization we may compare the indicator value (N) for both. This in case of identical material would lead to I_{varian} an index that could be used to quantify the level of gain in material utilization with respect to a reference configuration.

$$I_{varian} = \frac{N_n}{N_o} = \frac{(\rho v_n^2/E)}{(\rho v_o^2/E)} = \left(\frac{v_n}{v_o}\right)^2 = \frac{\omega_n^2}{\omega_o^2} \quad (4)$$

Which in the case of the same mass is a more justified measure for material utilization than the previously used “fundamental modal stiffness” ratio used in the previous section. Although, both indices (i.e., $I_{variant}$ in both cases) should give the same ratio for the same mass.

3.2 Perforation patterns

To rephrase the earlier question in terms of the currently adopted measure of material utilization. Could the material be redistributed with the same mass, and without changing the primary configuration to increase the material utilization of the structural subsystem? The hypothesis proposed here is that it is possible, and the current section will demonstrate the approach that was taken to test that hypothesis.

To illustrate how material redistribution is used to modify the ways in which materials behave, five shapes of perforations are used namely triangles, rectangles, diamonds, hexagons and Isogrid perforations, was used to study how “perforation pattern” affects the design efficacy of the plate. The concept of a “planar unit cell” is invoked here from the crystallography field. It is defined as a shape that is repeated regularly in the x and y directions of the cartesian plane to produce the pattern. To generate a bounded shape a specified number of repetitions of the geometric shape (unit cell) is used. The five candidate configurations for the purpose of comparison should have the same mass and same plate thickness. To achieve identical mass, the width of stiffeners was changed, however the overall plate area and plate thickness was maintained the same within the five candidates’ models as illustrated in Fig. 12.

For more discernable effect of the perforation pattern, each one of the five patterns described

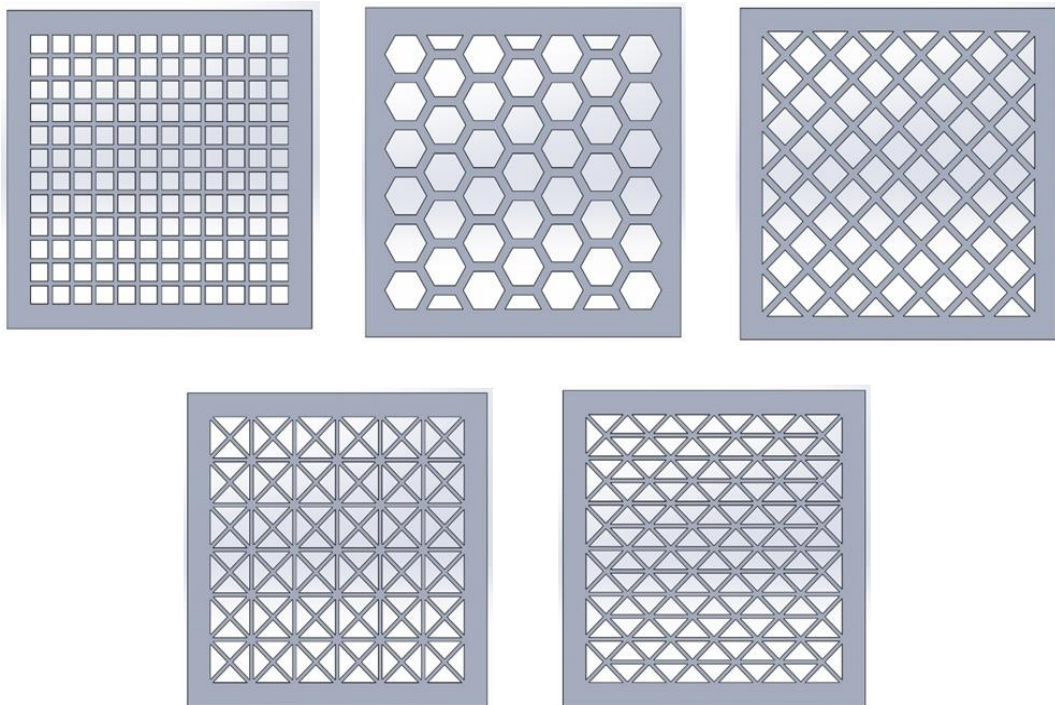


Fig. 12 Five shapes of perforations (triangles, rectangles, diamonds, hexagons and Isogrid)

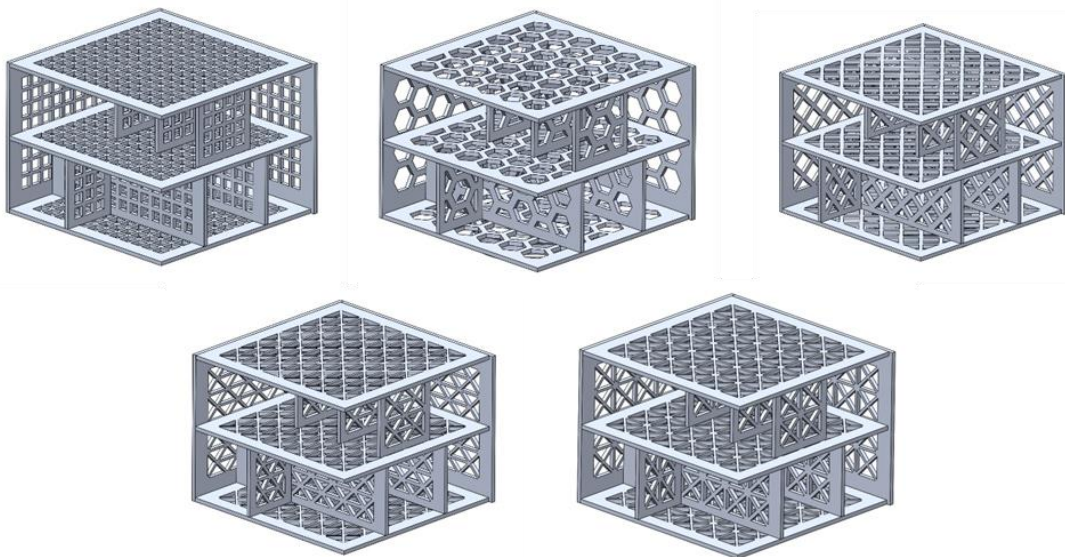


Fig. 13 CAD Models for five models of one group

above, was replicated five times using different plate thickness. So, now we have twenty-five models divided into five groups, each group have the same mass and plate thickness. Each group includes five models consisting of plates with the same thickness as shown in Fig. 13, but with

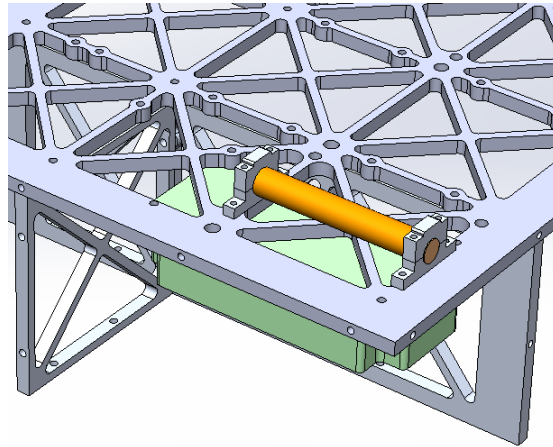


Fig. 14 “Perforation patterns” are suitable as platform of electronic parts

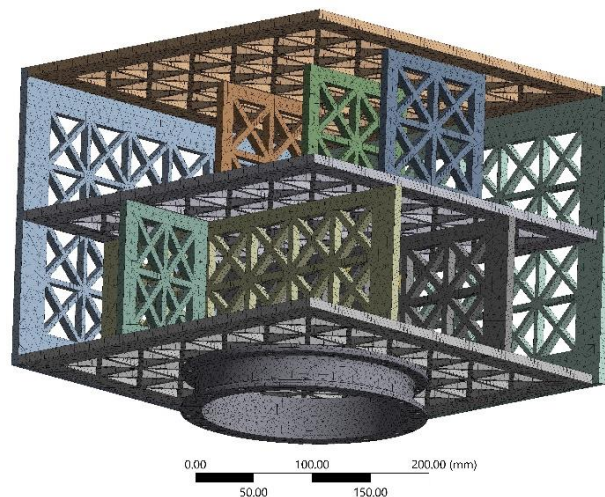


Fig. 15 Finite element meshing

different perforation shapes. This should eliminate any spurious improvement due to possible size effect Iqbal *et al.* (2022).

Fig. 14 shows how “Perforation patterns” are compatible with electronic subsystems, showing the magneto-torquer fixed on a unit cell in triangular perforated pattern. Area of grids around electronic parts connections were increased with round fillet to avoid stress concentration around connections.

4. FE model

To simulate the effect of the fasteners that firmly attach all parts of the structure assembly together, beam element connections were used. Beam element connections prevent any relative motion between the nodes and faces of adjacent parts. To simulate the attachment of the satellite

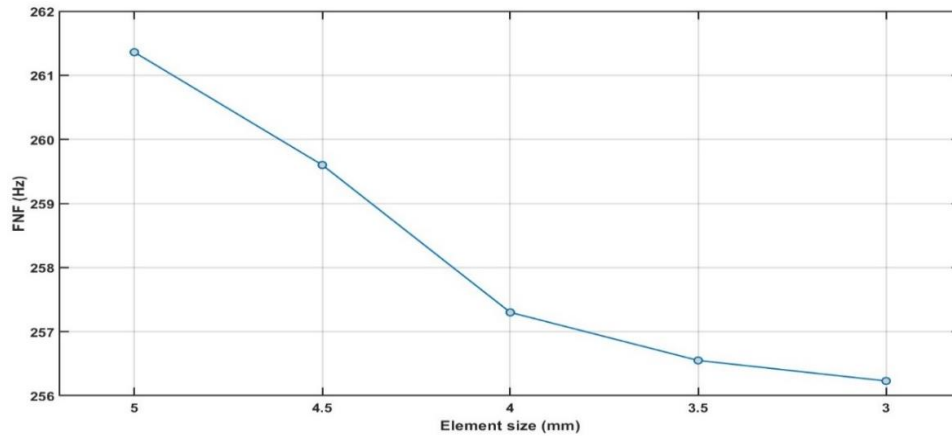


Fig. 16 Convergence study curves

with the launcher, fixed boundary conditions were imposed at the points of clamping between the separation adapter and the launcher, which is attached to the base plate of the satellite primary structure.

FE meshing of all the components was done using a second-order 10-node tetrahedral element, for high accuracy (illustrated in Fig. 15). Since the normal mode analysis is essentially a displacement analysis and the computational cost incurred by meshing using the high order hexahedral elements is not justified with respect to the accuracy benefit added, the second order tetrahedral element is more suitable for the current analysis. The mesh size was checked via a convergence study for all analyses presented in the current section, a representative sample of the convergence study curves are shown in Fig. 16.

As shown in Fig. 16, the number of elements in one of the configurations were increased gradually till no significant change in the FNF was detected. This minimum number of elements at which the FNF became constant is considered the converging mesh. Once the converging mesh size is established for each model of the 25 models studied, the values of FNFs, and its accompanying mode shapes, were used in computing the definitive measure for material utilization analysis $I_{variant}$.

In the following section we present the results of the normal modes analyses performed to compute the FNF and corresponding mode shapes for all the cases to be compared of the satellite structure.

5. Results and discussion

The study aimed to investigate the effect of different perforation patterns on the mass reduction and stiffness of microsatellite plates. In this study, five groups of perforated plates with the same mass and plate thickness were investigated. Fig. 17 shows the first mode shape for five models of one group. The perforation patterns in each group were arranged in different shapes of unit cells, and the results were arranged in columns based on the study group and in rows based on the shape of the perforation pattern as shown in Table 2.

To evaluate the correlation between the results and the plate thickness and perforation pattern,

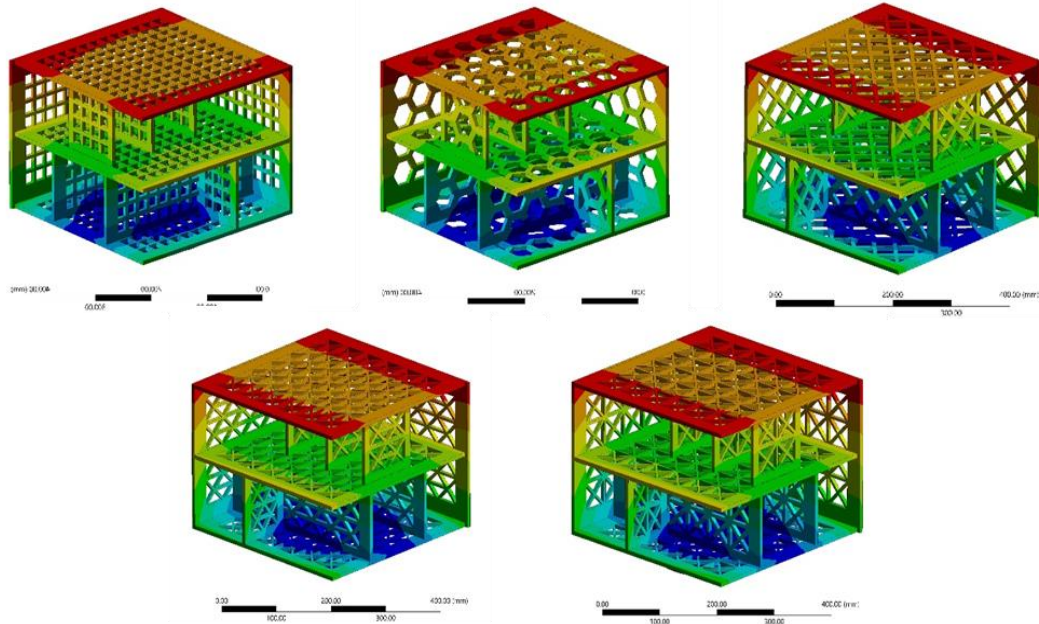


Fig. 17 First mode shape for five models of one group

Table 2 FNF and $I_{variant}$ of each perforation shape in five groups

		Rectangles	Hexagonal	Diamonds	Isogrid	Triangles
6 mm	FNF (Hz)	186.42	210.06	220.4	240.6	250.33
(9.02 Kg)	$I_{variant}$	-	1.27	1.40	1.67	1.80
7 mm	FNF (Hz)	198.9	217.87	226.35	245.9	256.55
(10.35 Kg)	$I_{variant}$	-	1.20	1.30	1.53	1.66
8 mm	FNF (Hz)	206.4	225.64	236.88	251.62	261.87
(11.65 Kg)	$I_{variant}$	-	1.20	1.32	1.49	1.61
9 mm	FNF (Hz)	212.75	231.56	243.82	256.8	267.54
(12.88Kg)	$I_{variant}$	-	1.18	1.31	1.46	1.58
10 mm	FNF (Hz)	217.51	238.98	252.12	261.91	273.32
(13.84 Kg)	$I_{variant}$	-	1.21	1.34	1.45	1.58

sensitivity analysis was conducted. The study found that the use of perforation patterns significantly reduced the mass of the microsatellite plates, with a mass reduction percentage of 39% compared to the unperforated configuration with the same plate thickness as shown in table 3. This percentage was higher than the percentages achieved in the previous studies mentioned in the introduction section. When compared to its baseline counterpart, the proposed perforated concept had a minimal impact on the overall characteristics of the FNF. However, it is worth noting that changes in natural frequencies are likely to occur due to the changes in mass and stiffness distribution caused by the implementation of the perforated concept. Additionally, it should be noted that the reduction percentage in FNF values is lower than the reduction in the overall mass ratio.

Table 3 FNF and Mass of 5 groups Vs. Un-perforated case

	6 mm Group	7 mm Group	8 mm Group	9 mm Group	10 mm Group
FNF (Hz) (unperforated)	310.2	319.32	329.16	385.42	360.6
FNF (Hz) (Triangles)	250.33	256.55	261.87	267.54	273.32
FNF reduction %	19%	20%	20%	31%	24%
Overall Mass (unperforated) (Kg)	14.7	16.9	18.9	21.1	22.7
Overall Mass (perforated) (Kg)	9.02	10.35	11.65	12.88	13.84
Mass reduction %	39%	39%	38%	39%	39%

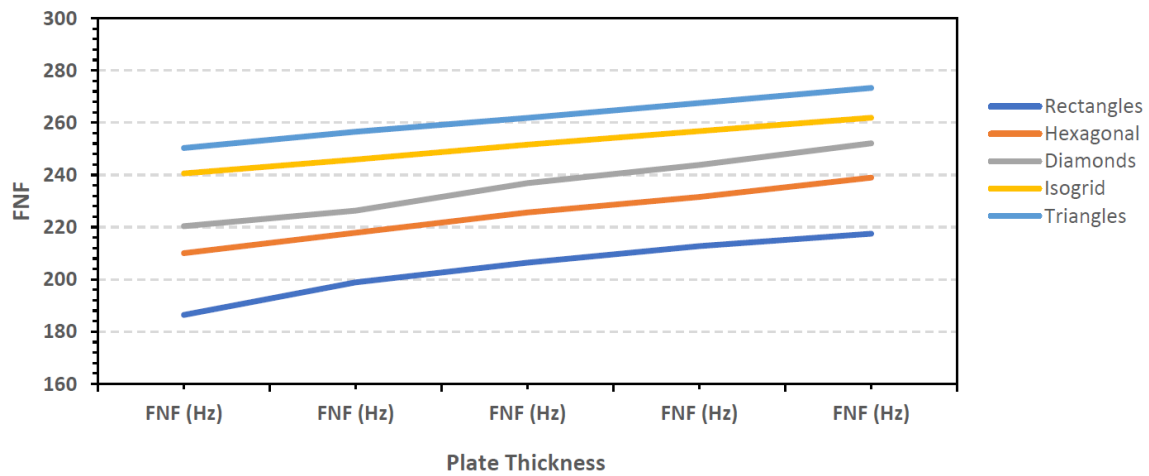


Fig. 18 Results (Shape Vs. Thickness Vs. FNF)

Also, the present study found that the use of different perforation patterns had varying effects on the values of FNF, which is a measure of the modal stiffness of the plate. The FNF values were affected differently based on the shape factor of the perforation pattern. The results showed that changing the perforation unit cell shapes during the conceptual design process could lead to better material utilization. Specifically, the adoption of triangular unit cells was found to be more effective than isogrid perforations in minimizing the mass of the microsatellite without sacrificing the stiffness.

The study found that the lowest material utilization efficiency, as quantified by the I-variant, were those of the rectangular perforation patterns, while the highest values were obtained via triangles patterns, So the finding agrees with the finding by Dawood *et al.* These finding depart from the commonly accepted paradigm that isogrid perforations are the best way to achieve the goal of minimizing mass while maintaining stiffness. The study highlights the potential benefits of exploring a wider range of perforation unit cells in the design process.

The results also suggest that similitude-based measures can provide a useful tool for evaluating material utilization in structural design. In this study, the sensitivity of FNF, i.e., I-variant, to the shape of the perforation pattern was found to be higher than the sensitivity to the thickness of the plate. Such a quantification approach is useful for designers, especially in the conceptual design phase.

To further analyze the results, Shape Vs. Thickness Vs. FNF was plotted in Fig. 18. The figure shows that FNF values, depending on the shape pattern factor, was similar in proportion across all

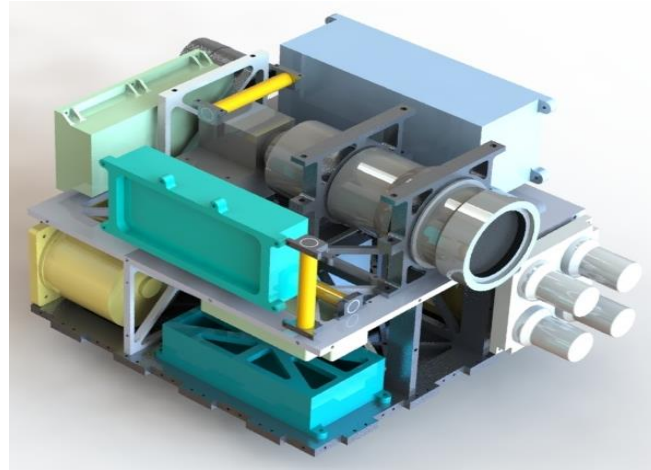


Fig. 19 Final configuration of the microsatellite

Table 4 Mass budget

SYBSYSTEM	Payload	Power	CDH	ADCS	COMUNICATION	STRUCTURE
Mass (Kg)	6.499	7.091	0.869	5.378	1.201	9.096
%	22%	24%	3%	18%	4%	30%
Total (Kg)	30.132					

groups in the current study. This supports the idea that the shape factor significantly affects FNF, i.e., I-variant.

Fig. 18 also revealed that the tendency to improve material utilization was more pronounced in thinner plates than in thicker plates. This result is practically relevant since lower thicknesses are typically preferred in the structural subsystem to lower the overall mass of the microsatellite. Therefore, by using perforation patterns with appropriate shapes, the material utilization efficiency of the microsatellite plates could be improved, resulting in a reduction in mass and better performance.

The configuration of variant 9 shown in Fig. 10 was used to develop the primary structural configuration and triangular perforation patterns were used to achieve minimum structural mass. All subsystems are accommodated inside this structure to satisfy the launch vehicle requirements. Moreover, some of these subsystems have its specific requirements which were considered. Fig. 19 shows the final configuration of the microsatellite including the payload and the bus subsystems components. Table 4 summarizes the mass budget of the payload and bus subsystems accommodated in the microsatellite structure.

6. Conclusions

The paper outlines a procedure for improving the material utilization of the structural subsystem of microsatellites, which involves two steps. The authors introduce a similitude-based measure for assessing the efficiency of different perforation unit cells in reducing the mass of the microsatellite while maintaining its stiffness. The study findings challenge the widely accepted

notion that isogrid perforations are the most effective way to achieve this goal, instead suggesting that the adoption of triangular unit cells at the conceptual design stage can result in a better material utilization. The results indicate that exploring a wider range of perforation unit cells during the design process may be beneficial, and that similitude-based measures can be a helpful tool in evaluating material utilization in structural design. To further establish the viability of the metal perforation pattern approach as a low-cost method for reducing the mass of astronautic systems, future work will investigate the structural performance of the mass-reduced structure under loads expected during the launch of the satellite into orbit, as well as thermal management in orbit. This would help to conclusively determine the effectiveness of the approach for achieving the desired mass reduction without compromising the performance.

Acknowledgement

The first author is grateful for the research support of the Egyptian space agency (EgSA).

References

- Abdelrahman, A.A., Eltaher, M.A., Kabeel, A.M., Abdraboh, A.M. and Hendi, A.A. (2019), "Free and forced analysis of perforated beams", *Steel Compos. Struct.*, **31**(5), 489. <https://doi.org/10.12989/scs.2019.31.5.489>.
- Aborehab, A., Kassem, M., Nemnem, A. and Kamel, M. (2019), "Miscellaneous modeling approaches and testing of a satellite honeycomb sandwich plate", *J. Appl. Comput. Mech.*, **6**, 1084-1097. <https://doi.org/10.22055/JACM.2019.31255.1846>.
- Aborehab, A., Kassem, M., Nemnem, A. and Kamel, M. (2021), "Mechanical characterization and static validation of a satellite honeycomb sandwich structure", *Eng. Solid Mech.*, **9**(1), 55-70. <https://doi.org/10.5267/j.esm.2020.5.004>.
- Akl, W., El-Sabbagh, A. and Baz, A. (2008), "Optimization of the static and dynamic characteristics of plates with isogrid stiffeners", *Finite Elem. Anal. Des.*, **44**(8), 513-523. <https://doi.org/10.1016/j.finel.2008.01.015>.
- Almitani, K.H., Abdelrahman, A.A. and Eltaher, M.A. (2020), "Influence of the perforation configuration on dynamic behaviors of multilayered beam structure", *Struct.*, **28**, 1413-1426. <https://doi.org/10.1016/j.istruc.2020.09.055>.
- Anonymous (2014), Cubesat Design Specification Rev 14, California Polytechnic State University.
- Anwar, A., Albano, M., Hassan, G., Delfini, A., Volpini, F., Marchetti, M. and Elfiky, D. (2015, May), "Vacuum effect on spacecraft structure materials", *International Conference on Aerospace Sciences and Aviation Technology*, **16**, The Military Technical College, May.
- Centea, T. and Nutt, S.R. (2016), "Manufacturing cost relationships for vacuum bag-only prepreg processing", *J. Compos. Mater.*, **50**(17), 2305-2321. <https://doi.org/10.1177/0021998315602949>.
- Cho, H.K. and Rhee, J. (2011), "Vibration in a satellite structure with a laminate composite hybrid sandwich panel", *Compos. Struct.*, **93**(10), 2566-2574. <https://doi.org/10.1016/j.compstruct.2011.04.019>.
- Cunningham, S.M., Tanner, D.A., Clifford, S., Butan, D. and Southern, M. (2020), "Effect of perforations on resonant modes of flat circular plates", *Key Eng. Mater.*, **865**, 31-35. <https://doi.org/10.4028/www.scientific.net/KEM.865.31>.
- Dawood, S.D.S. and Harmin, M.Y. (2022), "Structural responses of a conceptual microsatellite structure incorporating perforation patterns to dynamic launch loads", *Aerosp.*, **9**(8), 448. <https://doi.org/10.3390/aerospace9080448>.
- Dawood, S.D.S., Harithuddin, A.S.M. and Harmin, M.Y. (2022), "Modal analysis of conceptual

- microsatellite design employing perforated structural components for mass reduction”, *Aerosp.*, **9**(1), 23. <https://doi.org/10.3390/aerospace9010023>.
- Dawood, S.D.S., Harmin, M.Y., Harithuddin, A.S.M., Ciang, C.C. and Rafie, A.S.M. (2021), “Computational study of mass reduction of a conceptual microsatellite structural subassembly utilizing metal perforations”, *J. Aeronaut. Astronaut. Aviat.*, **53**, 57-66. [https://doi.org/10.6125/JoAAA.202103_53\(1\).05](https://doi.org/10.6125/JoAAA.202103_53(1).05).
- Desnoyers, N., Goyette, P., Leduc, B. and Boucher, M.A. (2017, September), “Dimensional stability performance of a CFRP sandwich optical bench for microsatellite payload”, *Material Technologies and Applications to Optics, Structures, Components, and Sub-Systems III*, **10372**, 96-105.
- Drenthe, N.T., Zandbergen, B.T.C., Curran, R. and Van Pelt, M.O. (2019), “Cost estimating of commercial smallsat launch vehicles”, *Acta Astronautica*, **155**, 160-169. <https://doi.org/10.1016/j.actaastro.2018.11.054>.
- Fakoor, M., Zadeh, P.M. and Eskandari, H.M. (2017), “Developing an optimal layout design of a satellite system by considering natural frequency and attitude control constraints”, *Aerosp. Sci. Technol.*, **71**, 172-188. <https://doi.org/10.1016/j.ast.2017.09.012>.
- Formisano, A., Lombardi, L. and Mazzolani, F.M. (2016), “Perforated metal shear panels as bracing devices of seismic-resistant structures”, *J. Constr. Steel Res.*, **126**, 37-49. <https://doi.org/10.1016/j.jcsr.2016.07.006>.
- García-Pérez, A., Sanz-Andrés, Á., Alonso, G. and Manguán, M.C. (2019), “Dynamic coupling on the design of space structures”, *Aerosp. Sci. Technol.*, **84**, 1035-1048. <https://doi.org/10.1016/j.ast.2018.11.045>.
- Ghonasgi, K., Bakal, K. and Mali, K.D. (2016), “A Parametric study on free vibration of multi-perforated rectangular plates”, *Procedia Eng.*, **144**, 60-67. <https://doi.org/10.1016/j.proeng.2016.05.007>.
- Guo, J., Zhang, J., Feng, Y., Wang, F. and Li, C. (2021), “Lightweight implementation of natural vibration frequency adjustment of satellite structures by varying the structural stiffness”, *Aerosp. Sci. Technol.*, **118**, 107061. <https://doi.org/10.1016/j.ast.2021.107061>.
- Hamid, Z.A., Mostafa, M.A., Abou El Khair, M.T., Gomaa, M.H., Elfiky, D. and Ahmed, A. (2022), “Casting and forming of nano hard aluminum oxide film on the modified 6061 Al alloys for NARSSCube satellite structure”, *Egypt. J. Remote Sens. Space Sci.*, **25**(4), 929-939. <https://doi.org/10.1016/j.ejrs.2022.09.002>.
- Heidt, H., Puig-Suari, J., Moore, A., Nakasuka, S. and Twiggs, R. (2000), “CubeSat: A new generation of picosatellite for education and industry low-cost space experimentation”, *AIAA/USU Conference on Small Satellites*, Utah State University, Logan, Utah.
- Iqbal, S., Jamil, T. and Mehdi, S.M. (2023), “Numerical simulation and validation of MWCNT-CFRP hybrid composite structure in lightweight satellite design”, *Compos. Struct.*, **303**, 116323. <https://doi.org/10.1016/j.compstruct.2022.116323>.
- Jeong, K.H. and Jhung, M.J. (2017), “Free vibration analysis of partially perforated circular plates”, *Procedia Eng.*, **199**, 182-187. <https://doi.org/10.1016/j.proeng.2017.09.230>.
- Jones, H. (2018), “The future impact of much lower launch cost”, *48th International Conference on Environmental Systems*, Albuquerque, NM, July.
- Kramer, H.J. and Cracknell, A.P. (2008), “An overview of small satellites in remote sensing”, *Int. J. Remote Sens.*, **29**(15), 4285-4337. <https://doi.org/10.1080/01431160801914952>.
- Kuo, J.C., Hung, H.C., Mei-Yi, Y., Chia-Ray, C. and Lin, J. (2017), “Composite materials application on FORMOSAT-5 remote sensing instrument structure”, *Terres., Atmosph. Ocean. Sci.*, **28**(2), 1.
- Kwon, S.C., Son, J.H., Song, S.C., Park, J.H., Koo, K.R. and Oh, H.U. (2021), “Innovative mechanical design strategy for actualizing 80 kg-Class X-Band active SAR small satellite of S-STEP”, *Aerosp.*, **8**(6), 149. <https://doi.org/10.3390/aerospace8060149>.
- Lester, C. and Nutt, S. (2018), *Composite Materials: Advantages and Cost Factors*, Los Angeles, California, USA.
- Lim, J., You, C. and Dayyani, I. (2020), “Multi-objective topology optimization and structural analysis of periodic spaceframe structures”, *Mater. Des.*, **190**, 108552. <https://doi.org/10.1016/j.matdes.2020.108552>.

- Liu, L., Wang, X., Sun, S., Cao, D. and Liu, X. (2019), "Dynamic characteristics of flexible spacecraft with double solar panels subjected to solar radiation", *Int. J. Mech. Sci.*, **151**, 22-32. <https://doi.org/10.1016/j.ijmecsci.2018.10.067>.
- Lv, M., Sun, D.W., Pu, H. and Zhu, H. (2022), "A core-shell-satellite structured Fe₃O₄@ MIL-100 (Fe)@ Ag SERS substrate with adsorption, detection, degradation and recovery functionalities for selective detection of cationic dyes", *Microchem. J.*, **183**, 108137. <https://doi.org/10.1016/j.microc.2022.108137>.
- Meyer, R.R., Harwood, O.P., Harmon, M.B. and Orlando, J.I. (1973), *Isogrid Design Handbook*, No. MFS-22686.
- Ontac, S., Dag, S. and Gokler, M.I. (2007), "Structural finite element analysis of stiffened and honeycomb panels of the RASAT satellite", *2007 3rd International Conference on Recent Advances in Space Technologies*, 171-175. <https://doi.org/10.1109/RAST.2007.4283971>.
- Pahl, G., Beitz, W., Feldhusen, J. and Grote, K.H. (2007), *Engineering Design: A Systematic Approach*, 3rd Edition, Springer.
- Sailesh, R., Yuvaraj, L., Pitchaimani, J., Doddamani, M. and Chinnapandi, L.B.M. (2021), "Acoustic behaviour of 3D printed bio-degradable micro-perforated panels with varying perforation cross-sections", *Appl. Acoust.*, **174**, 107769. <https://doi.org/10.1016/j.apacoust.2020.107769>.
- Salem, H., Boutchicha, D. and Boudjemai, A. (2018), "Modal analysis of the multi-shaped coupled honeycomb structures used in satellites structural design", *Int. J. Interact. Des. Manuf.*, **12**(3), 955-967. <https://doi.org/10.1007/s12008-017-0444-6>.
- Sarafin, T.P. and Larson, W.J. (1995). *Spacecraft Structures and Mechanisms: from Concept to Launch*, Microcosm Press and Kluwer Academic Publishers, Torrance.
- Shama Rao, N., Simha, T.G.A., Rao, K.P. and Ravi Kumar, G.V.V. (2018), "Carbon composites are becoming competitive and cost effective", White Paper.
- Spaceflight Inc. (2019), *Spaceflight Mission Planning Guide*, Spaceflight, Inc., Seattle, WA, USA.
- Stevens, C.L. (2002), "Design, analysis, fabrication, and testing of a nanosatellite structure", Doctoral Dissertation, Virginia Tech., Virginia.
- Sun, D.G., Guo, J.J., Song, Y., Yan, B.J., Li, Z.L. and Zhang, H.N. (2019), "Flutter stability analysis of a perforated damping blade for large wind turbines", *J. Sandw. Struct. Mater.*, **21**(3), 973-989. <https://doi.org/10.1177/1099636217705290>.
- Sweeting, M.N. (2018), "Modern small satellites-changing the economics of space", *Proc. IEEE*, **106**(3), 343-361. <https://doi.org/10.1109/JPROC.2018.2806218>.
- Viviani, A., Iuspa, L. and Arovitola, A. (2017), "Multi-objective optimization for re-entry spacecraft conceptual design using a free-form shape generator", *Aerosp. Sci. Technol.*, **71**, 312-324. <https://doi.org/10.1016/j.ast.2017.09.030>.
- Wagih, A.M., Hegaze, M.M. and Kamel, M.A. (2017), "FE modeling of Satellite's honeycomb sandwich panels using shell approach and solid approach", *AIAA SPACE and Astronautics Forum and Exposition*, 5184. <https://doi.org/10.2514/6.2017-5184>.
- Wei, J., Cao, D., Wang, L., Huang, H. and Huang, W. (2017), "Dynamic modeling and simulation for flexible spacecraft with flexible jointed solar panels", *Int. J. Mech. Sci.*, **130**, 558-570. <https://doi.org/10.1016/j.ijmecsci.2017.06.037>.
- Wu, C., Viquerat, A. and Aglietti, G. (2015), "Improving the natural frequency of bistable carbon fibre reinforced plastic tubes for space applications", *J. Int. Assoc. Shell Spatial Struct.*, **56**(4), 259-267.
- Xue, Y., Li, Y., Guang, J., Zhang, X. and Guo, J. (2008), "Small satellite remote sensing and applications—history, current and future", *Int. J. Remote Sens.*, **29**(15), 4339-4372. <https://doi.org/10.1080/01431160801914945>.
- Zhengchun, D., Mengrui, Z., Zhiguo, W. and Jianguo, Y. (2016), "Design and application of composite platform with extreme low thermal deformation for satellite", *Compos. Struct.*, **152**, 693-703. <https://doi.org/10.1016/j.compstruct.2016.05.073>.